Superconducting critical temperature and the isotope exponent versus total electron concentration for two-band superconductors: Effect of the band structure

J. J. Rodríguez-Núñez*
SUPERCOMP Laboratory, Departamento de Física–FACYT, University of Carabobo, Valencia, Venezuela

A. A. Schmidt†
Departamento de Matemática–UFSM, 97105-900 Santa Maria, RS, Brazil

(Received 23 January 2003; published 15 December 2003)

We consider the superconducting critical temperature T_c and the isotope exponent α versus carrier concentration ρ using the one-particle Green functions of the simplest coupled Hamiltonian for the two-band model with a single T_c [N. Kristoffel and P. Rubin, Physica C **356**, 171 (2001)]. One of the bands, $\varepsilon_2(\vec{k})$, is taken to be two dimensional, while the second band $\varepsilon_3(\vec{k})$ is taken to be three dimensional. Taking only nearest-neighbor hopping for each one of the bands, we obtain that T_c versus ρ is symmetric around half filling in agreement with a general theorem of quantum mechanics. We also obtained the chemical potential μ versus ρ for several values of attractive interaction. We find that (1) the superconducting critical temperature T_c is maximum at $\rho=1/2$; (2) the chemical potential remains basically inside the smaller band, for the range of carrier concentration and Debye frequencies considered; (3) the isotope exponent has several symmetric minima around half filling depending on the anisotropy of the three-dimensional tight-binding band, namely, $\gamma \equiv t_{3,x}/t_{3,z} \neq 1$; (4) the chemical-potential curves, namely, μ versus ρ are completely independent of pairing interaction and Debye frequency; and (5) the number of symmetric minima and T_c^{max} goes down with increasing t_3/t_2 ratio. We have briefly discussed the possible relevance of our results with recent experimental data of the two-band compound MgB_2.

DOI: 10.1103/PhysRevB.68.224512 PACS number(s): 74.20.Fg, 74.10.+v, 74.25.−q, 74.72.−h

I. INTRODUCTION

It was during the year 2001 that physicists[1] were stunned by the announcement that magnesium diboride MgB_2, a material known since the 1950's, superconducts[2] at a critical temperature T_c of 39 K. The superconductivity in MgB_2 has revived much interest in diboride systems within the physics community due to the simplicity of this compound. It has a hexagonal AlB_2-type crystal structure where the boron atoms form graphite-like sheets separated by hexagonal layers of Mg atoms. Unlike other superconductors, there are no complications as a result of *d* or *f* electrons, no spin degrees of freedom, and no structural phase transitions. All this makes MgB_2 an ideal system to test various theories of superconductivity from first-principles calculations. According to many authors, these conditions are believed to be the reason why this compound has a high-temperature. Additionally to the characteristics previously discussed, this material is interesting because of the following features: (1) it is made of very light and cheap elements; (2) it is a good metal where there is no high contact resistance between the grain boundaries, eliminating the weak-link problem that has avoided widespread commercialization of the high temperature superconductor (HTSC) cuprates; and (3) the conduction-electron density and normal-state conductivity are one to two orders of magnitude higher for this compound than the (HTSC) cuprates used in present day wires.

The electronic calculations of An and Picket[3] and others indicate that the bands near the Fermi surface arise mainly from the $p_{x,y}$ σ-bonding orbitals of B which are partially occupied. Yildirim and co-workers[4] and Mazin's group[5] point out that the in-plane modes are strongly coupled to B σ bands. This coupling can also be observed from the splitting of the B σ bands with the E_{2g} phonons. Other bands are not affected by these phonons. Joas *et al.*[6] have put forward a theory for phonon-induced superconductivity in MgB_2 by associating the low vibration mode ($\omega_\pi = 24$ meV and $\lambda_\pi = 1.4$) to the π states and the high vibration mode ($\omega_\sigma = 67$ meV and $\lambda_\sigma = 0.7$) to the σ states within the Eliashberg formalism. In their theory, the low-energy modes have the bigger spectral weight in the density of states, namely, $\lambda_\pi > \lambda_\sigma$. They are able to explain the critical-field anisotropy (tunneling experiments) of $H_{c_2}^{ab}/H_{c_2}^{c} \approx 3.9$. Recently, the Berkeley group[7] has explained the origin of the anomalous superconducting properties of MgB_2 by means of an *ab initio* calculation of the superconducting gaps and their effects on measurable quantities, such as the anomalous structure of the specific heat.

We adopt as a microscopic Hamiltonian the following:[8]

$$H = \sum_{k,\sigma} \epsilon_2(\vec{k}) n_{s,\vec{k}} + \sum_{k,\sigma} \epsilon_3(\vec{k}) n_{d,\vec{k}} - V \sum_{\vec{k},\vec{k'}} (c^{\dagger}_{\vec{k},\uparrow} c^{\dagger}_{-\vec{k},\downarrow} d_{-\vec{k'},\downarrow} d_{\vec{k'},\uparrow} + d^{\dagger}_{\vec{k},\uparrow} d^{\dagger}_{-\vec{k},\downarrow} c_{-\vec{k'},\downarrow} c_{\vec{k'},\uparrow}), \tag{1}$$

where $\epsilon_2(\vec{k})$ and $\epsilon_3(\vec{k})$ are the band structures of the two bands; $V \geqslant 0$ is the averaged interaction energy resulting from phonon emission and absorption by *s-d* processes, minus the corresponding shielded Coulomb interaction

term;[8–12] $n_{2,\vec{k}}=c^{\dagger}_{\vec{k}}c_{\vec{k}}$, with c_σ the annihilation operator for the 2-band, etc. In Eq. (1) we have taken $V_{22}=V_{33}=0$ (Refs. 8–12) for simplicity. We would like to say that in the MgB_2 compound, $V_{22},V_{33}>V_{23}=V$. Because of this, our choice may consider MgB_2 only as a possible realization of a two-band superconductivity. Let us fix our notation. "2" or "s" means the two-dimensional band and "3" or "d" or "D" is reserved for the three-dimensional band.

According to different experimental probes,[13–19] this compound can be explained by using a two s-wave order-parameter superconductor. In particular we mention the microwave properties for c-axis films, with aligned samples, where a large gap is obtained, $\Delta_{ab}\approx 7.5$ meV, while in unaligned samples it is the small gap, $\Delta_c\approx 3$ meV, which determines the electrodynamic response.[20]

Yamaji[21] has used tight-binding modeling to explain a two-band-type superconducting instability in MgB_2. In particular, Yamaji[22] has used the tight-binding method for the π bands in MgB_2, together with the Hubbard on-site Coulomb interaction on two inequivalent boron p_z orbitals. He finds that the amplitude of interband pair scattering between two π bands diverges if the interband polarization function in it becomes large enough. These results lead to a divergent interband pair scattering, meaning two-band-type superconducting instability with enhanced T_c. Yamaji used the same type of arguments as Furukawa[22] who pointed out that the Fermi surfaces of the two π bands are close to perfect nesting. According to this mechanism T_c can go up further through improvement of the nesting.

Nakai, Ichioka, and Machida[23] have studied the magnetic-field dependence of electronic specific heat in two-band superconductors, namely, $\gamma(H)\propto H^{\alpha}$. They conclude that the observed extremely small value of $\alpha\approx 0.23$ could be reasonably explained by a two-band model.

However, there is another approach due to Maki and co-workers[24] and Mishonov *et al.*[25] which considers that the experimental data of MgB_2 can be explained by using a single anisotropic order-parameter superconductor. According to Haas and Maki,[24] two-gap model can have similar properties of the anisotropic s-wave model proposed by them, and therefore experimental tests to distinguish between these theories are highly desirable.

Additionally, this compound is considered a strong-coupling superconductor by Kortus and co-workers.[26] Moca[27] has calculated the penetration depth in MgB_2 using Eliashberg theory of superconductivity for two bands. It has also been considered a superconductor with nodes in the order parameter.[28] We mention that the present quest by experimentalists is to obtain pure samples.[29] Intense studies on polycrystalline samples have been done by de Lima *et al.*[30] See also Ref. 31.

We are going to consider a compound which can be described approximately by a two-band superconductor. We neglect in this paper strong-coupling effects, Coulomb repulsion, and anisotropic effects in the order parameters. Two-band superconductors are not restricted only to MgB_2. The two-band model has been also applied to high-T_c superconductors by Okoye[32] to explain the isotope effect of Y compounds. Shulga *et al.*[33] have used an effective two-band model to explain new upper critical field $H_{c\,2}(T)$ data in a broad temperature range $0.3K\leqslant T\leqslant T_c$ for $LuNi_2B_2C$ and YNi_2B_2C single crystals with well characterized low impurity scattering rates. For Sr_2RuO_4 we have a complex order parameter (OP), composed of Ru $4d_{xy}++\mathrm{Ru}\{4d_{xz},4d_{yz}\}$ bands.[34]

We finally add that the physical picture of this compound is not clearly understood. For example, Sologubenko *et al.*[35] have found that the Wiedemann-Franz law of the field-induced normal state at low temperatures, i.e., $T_c\approx 1$ K, is not satisfied due to an unexpected instability of the electronic subsystem. According to Yildirim[1] all controversial issues in this compound will be resolved when good quality large single crystal of MgB_2 are available for additional measurements.

This paper is organized as follows. In Sec. II, we give a derivation of the one-particle Green functions for the two bands in the superconducting state using the model Hamiltonian, Eq. (1). The one-particle Green functions are used to derive the order parameters $\Delta_{22}(T)$ and $\Delta_{33}(T)$ and the superconducting critical temperature T_c. In Sec. III we derive the two self-consistent equations at T_c, one for T_c and another one for ρ, the total carrier concentration/site/spin/band. These equations are solved numerically after performing the summation of the odd Matsubara frequencies. In Sec. IV we present our discussion and conclusions.

II. THE ONE-PARTICLE GREEN FUNCTIONS

Due to the fact that MgB_2 has a unique temperature, Eq. (1) captures the main physics of this compound. In other words, we are going to neglect the energies resulting from phonon emission and absorption by s-s and d-d processes, i.e., $V_{22}=V_{33}=0$. These terms can be included, but the physics is governed by the presence of the parameter $V\neq 0$. The order-parameter equations and T_c can be found using the method of Bogoliubov and Valatin.[36] However, as we are preparing the ground for several thermodynamic properties, we will follow the equation of motion approach for the operators $c_{\vec{k},\sigma}$ and $d_{\vec{k},\sigma}$. For example, for $c_{\vec{k},\sigma}$, it is given by[37,38]

$$\frac{\partial}{\partial\tau}c_{\vec{k},\sigma}=-\varepsilon_2(\vec{k})c_{\vec{k},\sigma}+\sigma V c^{\dagger}_{\vec{k},\sigma}\sum_{\vec{k}'}\ d_{-\vec{k}',\downarrow}d_{\vec{k}',\uparrow}\,. \qquad (2)$$

Similarly, we find

$$\frac{\partial}{\partial\tau}d_{\vec{k},\sigma}=-\varepsilon_3(\vec{k})d_{\vec{k},\sigma}+\sigma V d^{\dagger}_{\vec{k},\sigma}\sum_{\vec{k}'}\ c_{-\vec{k}',\downarrow}c_{\vec{k}',\uparrow}\,. \qquad (3)$$

Next, we define the one-particle Green functions as follows:

$$G_{22}(\vec{k},\tau-\tau')\equiv-\langle T_\tau c_{\vec{k},\sigma}(\tau)c^{\dagger}_{\vec{k},\sigma}(\tau')\rangle;$$

$$G_{33}(\vec{k},\tau-\tau')\equiv-\langle T_\tau d_{\vec{k},\sigma}(\tau)d^{\dagger}_{\vec{k},\sigma}(\tau')\rangle;$$

$$F_{22}^{\dagger}(\vec{k},\tau-\tau') \equiv \langle T_{\tau} c_{\vec{k},\uparrow}^{\dagger}(\tau) c_{-\vec{k},\downarrow}^{\dagger}(\tau')\rangle;$$

$$F_{33}^{\dagger}(\vec{k},\tau-\tau') \equiv \langle T_{\tau} d_{\vec{k},\uparrow}^{\dagger}(\tau) d_{-\vec{k},\downarrow}^{\dagger}(\tau')\rangle. \quad (4)$$

In Eq. (4), T_{τ} means the usual imaginary time ordering. From the definition of the one-particle Green functions, Eq. (4), and using the time evolution of creation and annihlation operators, Eqs. (2) and (3), we obtain dynamics for the one-particle Green functions:

$$\frac{\partial}{\partial\tau} G_{22}(\vec{k},\tau-\tau') = \delta_{\tau,\tau'} - \varepsilon_2(\vec{k}) G_{22}(\vec{k},\tau-\tau') - \sigma V \sum_{\vec{k}'} \langle T_{\tau}[c_{-\vec{k},\bar{\sigma}}^{\dagger}(\tau) d_{-\vec{k}',\downarrow}(\tau) d_{\vec{k}',\uparrow}(\tau) c_{\vec{k},\sigma}^{\dagger}(\tau)]\rangle, \quad (5)$$

$$\frac{\partial}{\partial\tau} F_{22}^{\dagger}(\vec{k},\tau-\tau') = \varepsilon_2(\vec{k}) F_{22}^{\dagger}(\vec{k},\tau-\tau') - V \sum_{\vec{k}'} \langle T_{\tau}[d_{\vec{k}',\uparrow}^{\dagger}(\tau) d_{-\vec{k}',\downarrow}^{\dagger}(\tau) c_{-\vec{k},\downarrow}^{\dagger}(\tau) c_{-\vec{k},\downarrow}^{\dagger}(\tau')]\rangle. \quad (6)$$

By Fourier transforming Eqs. (5) and (6) and adopting a decoupling scheme at the mean-field level, we end up with the set of coupled equations

$$[i\omega_n - \varepsilon_2(\vec{k})] G_{22}(\vec{k},i\omega_n) + \Delta_{33}(T) F_{22}^{\dagger}(\vec{k},i\omega_n) = 1,$$

$$-[i\omega_n + \varepsilon_2(\vec{k})] F_{22}^{\dagger}(\vec{k},i\omega_n) = \Delta_{33}^{*}(T) G_{22}(\vec{k},i\omega_n), \quad (7)$$

whose solutions are

$$G_{22}(\vec{k},i\omega_n) = \frac{i\omega_n + \varepsilon_2(\vec{k})}{[i\omega_n - \varepsilon_2(\vec{k})][i\omega_n + \varepsilon_2(\vec{k})] - |\Delta_{33}(T)|^2},$$

$$F_{22}^{\dagger}(\vec{k},i\omega_n) = \frac{-\Delta_{33}^{*}(T)}{[i\omega_n - \varepsilon_2(\vec{k})][i\omega_n + \varepsilon_2(\vec{k})] - |\Delta_{33}(T)|^2}. \quad (8)$$

In Eqs. (7) and (8), $\omega_n \equiv (2n+1)\pi T$ are the odd Matsubara frequencies, with T the absolute temperature and $n = 0,1,2,\ldots$. Similarly, we find that

$$G_{33}(\vec{k},i\omega_n) = \frac{i\omega_n + \varepsilon_3(\vec{k})}{[i\omega_n - \varepsilon_3(\vec{k})][i\omega_n + \varepsilon_3(\vec{k})] - |\Delta_{22}(T)|^2},$$

$$F_{33}^{\dagger}(\vec{k},i\omega_n) = \frac{-\Delta_{22}^{*}(T)}{[i\omega_n - \varepsilon_3(\vec{k})][i\omega_n + \varepsilon_3(\vec{k})] - |\Delta_{22}(T)|^2}. \quad (9)$$

To calculate $\Delta_{22}^{*}(T)$ and $\Delta_{33}^{*}(T)$ we must use the definition of these self-consistent parameters, namely,

$$\Delta_{22}(T) \equiv \frac{VT}{N_2} \sum_{\vec{k},i\omega_n} F_{22}^{*}(\vec{k},i\omega_n),$$

$$\Delta_{33}(T) \equiv \frac{VT}{N_3} \sum_{\vec{k},i\omega_n} F_{33}^{*}(\vec{k},i\omega_n), \quad (10)$$

giving the following results:

$$\Delta_{22}^{*}(T) = -V\Delta_{33}^{*}(T) \frac{T}{N_2} \times \sum_{\vec{k},i\omega_n} \frac{1}{[i\omega_n - \varepsilon_2(\vec{k})][i\omega_n + \varepsilon_2(\vec{k})] - |\Delta_{33}(T)|^2}, \quad (11)$$

$$\Delta_{33}^{*}(T) = -V\Delta_{22}^{*}(T) \frac{T}{N_3} \times \sum_{\vec{k},i\omega_n} \frac{1}{[i\omega_n - \varepsilon_3(\vec{k})][i\omega_n + \varepsilon_3(\vec{k})] - |\Delta_{22}(T)|^2}, \quad (12)$$

where $N_2 = N_x \times N_y$ and $N_3 = N_x \times N_y \times N_z$ is the number of lattice sites. As pointed out before, the 2-band is two dimensional, while the 3-band is three dimensional. In our discrete calculations we have set $N_x = N_y = N_z = 1024$.

At the same time, the charge-carrier densities ρ_2 and ρ_3 are calculated from the following expressions:

$$\rho_2 = \frac{T}{N_2} \sum_{\vec{k},i\omega_n} \frac{i\omega_n + \varepsilon_2(\vec{k})}{[i\omega_n - \varepsilon_2(\vec{k})][i\omega_n + \varepsilon_2(\vec{k})] - |\Delta_{33}(T)|^2},$$

$$\rho_3 = \frac{T}{N_3} \sum_{\vec{k},i\omega_n} \frac{i\omega_n + \varepsilon_3(\vec{k})}{[i\omega_n - \varepsilon_3(\vec{k})][i\omega_n + \varepsilon_3(\vec{k})] - |\Delta_{22}(T)|^2}. \quad (13)$$

In Sec. III we derive the two self-consistent equations we have to solve when $T = T_c$. We also present the two tight-binding band structures we are going to consider.

III. SELF-CONSISTENT EQUATIONS AT $T = T_c$

Combining the previous Eqs. (11) and (12) we get the following self-consistent equation:

$$\frac{1}{V^2} = F_2(\Delta_{33}) F_3(\Delta_{22}), \quad (14)$$

where $F_2(\Delta_{33})$ and $F_3(\Delta_{22})$ are given by

$$F_2(\Delta_{33}) \equiv \sum_{\vec{k},i\omega_n} \frac{T/N_2}{[i\omega_n - \varepsilon_2(\vec{k})][i\omega_n + \varepsilon_2(\vec{k})] - |\Delta_{33}(T)|^2},$$

$$F_3(\Delta_{22}) \equiv \sum_{k,i\omega_n} \frac{T/N_3}{[i\omega_n - \varepsilon_3(\vec{k})][i\omega_n + \varepsilon_3(\vec{k})] - |\Delta_{22}(T)|^2}. \tag{15}$$

From Eqs. (11) and (12) we see that if $\Delta_{22}=0$, so is Δ_{33}. This is again a realization that we have a unique superconducting critical temperature T_c. This can be calculated by selecting $\Delta_{22}(T_c)=\Delta_{33}(T_c)=0$. This yields

$$T_c = \frac{2e^{\gamma}}{\pi}\frac{\hbar\omega_D}{k_B}\exp\left\{-\frac{1}{V[N_{o,s}N_{o,d}]^{1/2}}\right\}, \tag{16}$$

which is the classical result obtained by Suhl, Matthias, and Walker[8] many years ago. $N_{o,2}$ and $N_{o,3}$ are the density of states of the bands 2 and 3, respectively.

However, in this paper, we will solve Eq. (14), at $T=T_c$, taking into consideration the chemical potential μ. This is taken in the usual way, namely, $\varepsilon_{2,3}(\vec{k})=\epsilon_{2,3}-\mu$, where

$$\epsilon_2 \equiv -2t_2[\cos(k_x)+\cos(k_y)-2\alpha'\cos(k_x)\cos(k_y)],$$

$$\epsilon_2 \equiv -2t_3[\cos(k_x)+\cos(k_y)+\gamma\cos(k_z)], \tag{17}$$

where t_2 is the hopping integral between nearest neighbors (nn's) in the two-dimensional band and t_3 is the hopping integral between nearest neighbors in the three-dimensional band. For simplicity, we are taking all nn hopping integrals equal to each other, for the two-dimensional band, namely, $t_{2,x}=t_{2,y}=t_2$ and, also, $\alpha'=0$. For the three-dimensional band we have parametrized as follows: $t_{3,x}=t_{3,y}$ and $t_{3,z}=\gamma t_{3,x}=t_3$. In the following calculations we have adopted that the two bands have the same hopping integral, namely, $t_2=t_3$. This choice was taken by Yamaji in Ref. 21. At $T=T_c$, Eqs. (15) become

$$F_2(0)=\frac{1}{N_2}\sum_{\vec{k}}\frac{\tanh[\varepsilon_2(\vec{k})/2T_c]}{2\varepsilon_2(\vec{k})},$$

$$F_3(0)=\frac{1}{N_3}\sum_{\vec{k}}\frac{\tanh[\varepsilon_3(\vec{k})/2T_c]}{2\varepsilon_3(\vec{k})}. \tag{18}$$

After performing the odd Matsubara summation for Eq. (12), at $T=T_c$, we arrive at the following equation for the total carrier concentration/site/spin/band, $\rho \equiv (\rho_2+\rho_3)/2$:

$$\rho = \tfrac{1}{2} - \tilde{F}_2(0) - \tilde{F}_3(0),$$

$$\tilde{F}_2(0)=\frac{1}{4N_2}\sum_{\vec{k}}\tanh\left(\frac{\varepsilon_2(\vec{k})}{2T_c}\right),$$

$$\tilde{F}_3(0)=\frac{1}{4N_3}\sum_{\vec{k}}\tanh\left(\frac{\varepsilon_3(\vec{k})}{2T_c}\right). \tag{19}$$

From Eq. (19), we immediately see that for $\mu=0$, we have $\rho=1/2$ (half filling), which is a theorem in quantum mechanics. This result tells us that in the Ginzburg-Landau expansion of Rodríguez-Núñez and co-workers,[39,40] their coefficients have been calculated at half filling, namely, $\mu \equiv 0$. Equation (19) allows us to calculate the carrier density of each of the bands.

IV. DISCUSSION, CONCLUSIONS, AND OUTLOOK

One of the great advantages of our set of Eqs. (14) and (19), at $T=T_c$, is that we can calculate the isotope effect (IE) for this model, which is a generalization of the work performed by de Mello and Rodríguez–Núñez.[41] Even when the IE is one of the most relevant effects produced by the electron-phonon interaction,[42] there are other observable effects as well. For example, Bill, Kresin, and Wolf[43] have discussed the isotope coefficient, as the London penetration depth λ_L, which depends on the phonon frequency ω_D. Our Eqs. (14) and (19), at $T=T_c$, have not been restricted to the neighborhood of the Fermi sea. When we impose that the pairing interaction is restricted to this neighborhood, we have to substitute $F_2(0)$ and $F_3(0)$ [Eqs. (18)] by the following expressions:

$$F_2(0)=\frac{1}{N_2}\sum_{\vec{k}}\frac{\chi(\vec{k})\tanh[\varepsilon_2(\vec{k})/2T_c]}{2\varepsilon_2(\vec{k})},$$

$$F_3(0)=\frac{1}{N_3}\sum_{\vec{k}}\frac{\chi(\vec{k})\tanh[\varepsilon_3(\vec{k})/2T_c]}{2\varepsilon_2(\vec{k})}, \tag{20}$$

where $\chi(\vec{k})=1$ for $|\varepsilon_{2,3}| \leqslant \omega_D$ and $\chi(\vec{k})=0$ for $|\varepsilon_{2,3}| > \omega_D$. ω_D is the Debye frequency.

We mention that the electronic thermal conductivity κ_e of multiband superconductors with application to MgB_2 has been discussed by Kusunose, Rice, and Sigrist.[44] Their conclusion is that the remarkable field dependence of κ_e can be explained as a consequence of multigap superconductivity. They also consider that moderately clean samples are needed to explain the data.

A. Results using Eq. (18)

In Fig. 1, we present T_c versus ρ and μ versus ρ, for several values of the interaction potential V, with $\gamma=1.0$ and $\alpha'=0$ [see Eq. (17)]. We have numerically solved Eqs. (14) and (19), at $T=T_c$, taking into consideration the band structure of Eq. (17). These two equations have been solved using a parallel program in a cluster of four Pentium processors of 1 GHz each.

The key feature of this figure is the high symmetry around half filling. This is due to our choice of the two-band structures [Eq. (17)].

Naturally, we can include some more complex band structures, taking into consideration next-nearest-neighbor hopping ($\alpha' \neq 0$) and, also, $\gamma \neq 1.0$. The case of $\alpha' \neq 0$ is going to be discussed later on. The consideration of next nearest neighbor hopping has been proven to be important by Soares *et al.*,[45] for one-band superconductors with *d*-wave order parameter.

From the work of Buzea and Yamashita[31] it is concluded

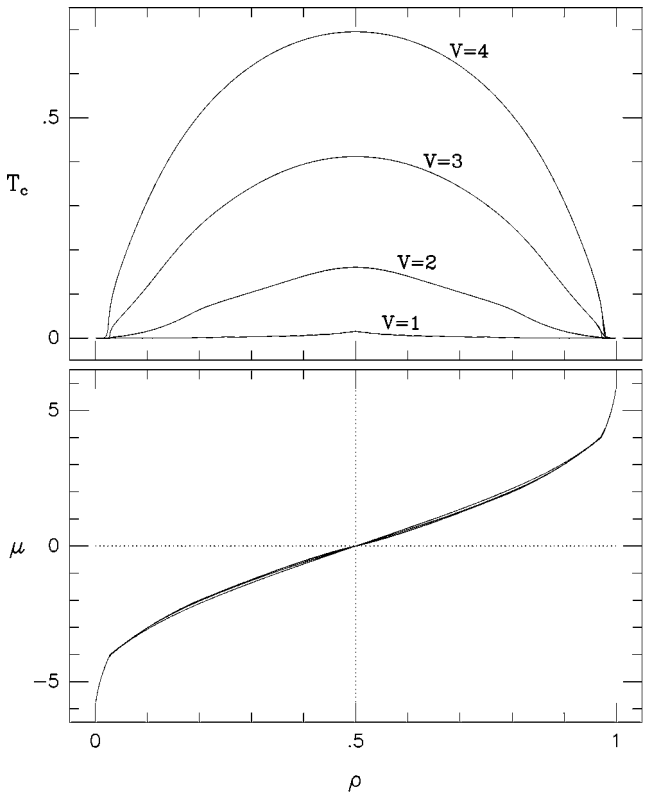

FIG. 1. The superconducting critical temperature T_c versus ρ, for several values of the attractive interaction V, namely, $V=1,2,3,4$ (upper panel). In the lower panel, we have the chemical potential, μ versus ρ, for the same values of the attractive interaction, V. We have taken $\gamma=1.0$ and $\alpha'=0.0$ [see Eq. (17)].

that MgB_2 is one member of a long list of binary, ternary, quaternary borides and borocarbides. MgB_2 has the highest T_c among all its family members. If we look at the results presented in Fig. 1 we conclude that the maximum T_c occurs at half filling. In consequence, according to the free tight-binding band structure chosen MgB_2 should be at half filling.

In the lower panel of Fig. 1 we have plotted μ versus ρ for different values of pairing potential, namely, $V=1,2,3,4$. We can see that the chemical potential is independent of V, i.e., the four curves are almost one on top of the other. Another aspect which we will like to stress is that the chemical potential almost stays inside the smaller band, the two-dimensional one. For example, for $0\leqslant\rho<0.05$ we have $-6.0\leqslant\mu<-4.0$.

B. Results using Eq. (20)

We want to consider the effect of the Debye frequency ω_D on T_c. As it is known the isotope exponent α is found from the following relation:

$$T_c\propto M^{-\alpha},\quad \omega_D\propto M^{-1/2}, \tag{21}$$

where M is the isotope ionic mass. For a single band in the weak BCS approximation, $T_c=1.14\omega_D\exp(-1/\lambda)$, where $\lambda\equiv N(0)V$ and $N(0)$ is the density of states at the Fermi sea. This yields $\alpha=1/2$. Furthermore, in the strong electron-phonon BCS model, T_c is given by[46]

$$T_c=\frac{\omega_D}{1.45}e^{-[1.04(1+\lambda)]/[\lambda-\mu^*(1+0.62\lambda)]}, \tag{22}$$

where μ^* is the Coulomb pseudopotential given by

$$\mu^*=\frac{N(0)V_c}{1+N(0)V_c\ln(E_B/\omega_D)}, \tag{23}$$

with V_c being the strength of the Coulomb interaction and E_B the energy interval where $V_c\neq 0$. Using Eq. (22) and the definition of the isotope exponent [Eq. (21)], we find in the McMillan approximation that

$$\alpha=\frac{1}{2}\left\{1-\left[\mu^*\ln\left(\frac{\Theta_D}{1.45T_c}\right)\right]^2\frac{1+0.62\lambda}{1+\lambda}\right\}. \tag{24}$$

By using the definition of the isotope exponent [Eq. (21)] with the two self-consistent equations [Eqs. (19) and (20)], we arrive at the following expression for the isotope exponent:

$$\alpha=-\frac{\frac{\omega_D}{2T_c}\left(F_2\frac{\partial F_1}{\partial\omega_D}+F_1\frac{\partial F_2}{\partial\omega_D}\right)}{D},$$

$$D\equiv F_2\frac{\partial F_1}{\partial T_c}+F_1\frac{\partial F_2}{\partial T_c}-D_m,$$

$$D_m=\frac{\left(F_2\frac{\partial F_1}{\partial\mu}+F_1\frac{\partial F_2}{\partial\mu}\right)\left(\frac{\partial\tilde{F}_1}{\partial T_c}+\frac{\partial\tilde{F}_2}{\partial T_c}\right)}{\frac{\partial\tilde{F}_1}{\partial\mu}+\frac{\partial\tilde{F}_2}{\partial\mu}}. \tag{25}$$

This is considered in Figs. 2 and 3, for different values of the Debye frequency ω_D. However, to speed up the calculations we have converted our sums to integrals, since the isotope exponent depends on the mesh number of points, N_x, N_y, N_z. For example, we have used the density of states in three dimensions given by

$$N_3(\epsilon)=C\int_l^L F(\pi/2,k(t))dt,$$

$$L=\arccos\{\max[-1,(\omega-2)/\gamma]\},\quad \omega=\frac{\epsilon}{2t_3},$$

$$l=\arccos\{\min[1,(\omega+2)/\gamma]\},\quad C=\frac{1}{2\pi^3t_2},$$

$$k(t)=\sqrt{1-\frac{[\omega-\gamma\cos(t)]^2}{4}}, \tag{26}$$

and $F(\pi/2,x)$ is the elliptic integral of the first kind. Our results [Eq. (26)] have been elaborated from that of Pesz and

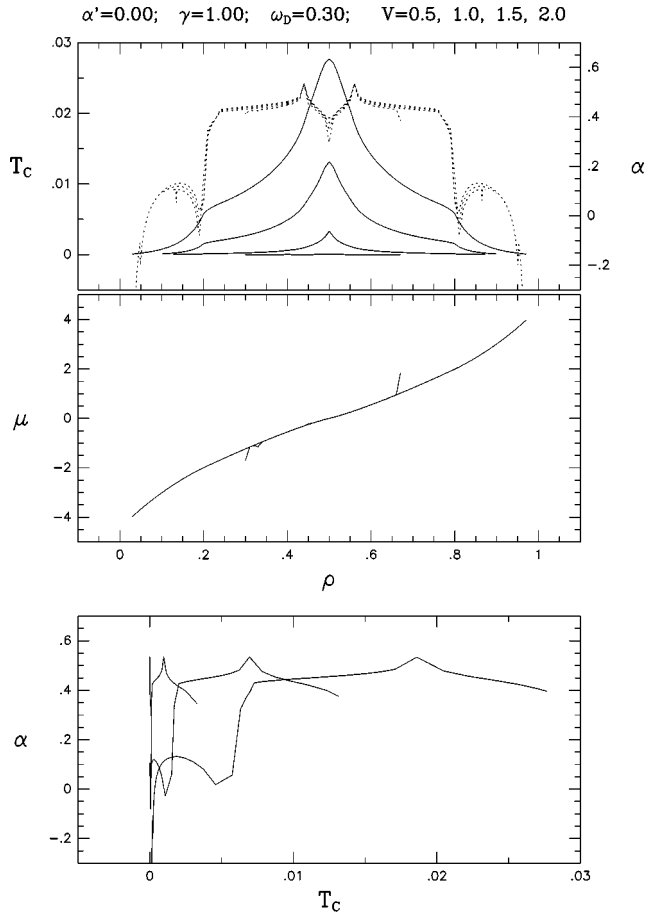

FIG. 2. The superconducting critical temperature T_c versus ρ, for several values of the attractive interaction V, namely, $V=0.5,1.0,1.5,2.0$ (upper panel, left scale) and the isotope exponent α versus ρ (upper panel, right scale). In the middle panel, we have the chemical potential μ versus ρ, for the same values of the attractive interaction V. We have taken $\gamma=1.0$ and $\alpha'=0.0$ [see Eq. (17)]. Here, we have used a Debye frequency $\omega_D=0.30$.

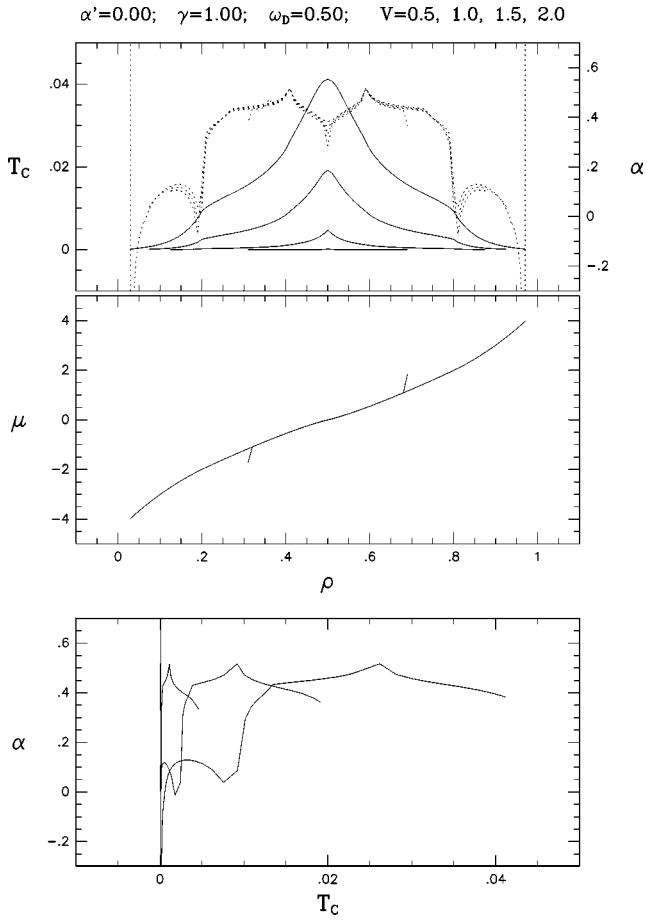

FIG. 3. The superconducting critical temperature T_c versus ρ, for several values of the attractive interaction V, namely, $V=0.5,1.0,1.5,2.0$ (upper panel, left scale) and the isotope exponent α versus ρ (upper panel, right scale). In the middle panel, we have the chemical potential μ versus ρ, for the same values of the attractive interaction V. We have taken $\gamma=1.0$ and $\alpha'=0.0$ [see Eq. (17)]. Here, we have used a Debye frequency $\omega_D=0.50$.

Munn.[47] In the case of the two dimensions, we have used the density of states $N_2(\epsilon)$ given by Kishine,[48] namely,

$$N_2(\epsilon)=\frac{1}{2\pi^2 t_2\sqrt{1+\alpha'\epsilon/t_2}}K\left(\sqrt{\frac{1-\left(\alpha'-\frac{\epsilon}{4t_2}\right)^2}{1+\alpha'\epsilon/t_2}}\right), \tag{27}$$

where $K(x)=F(\pi/2,x)$ is the elliptic integral of the first kind. For example, for the case of Eq. (20), we can rewrite $F_2(0)$ as follows:

$$F_2(0)=\frac{1}{2}\int_{l_2}^{L_2}\frac{N_2(\epsilon)\tanh\left(\frac{\epsilon-\mu}{2T_c}\right)}{\epsilon-\mu},$$

$$L_2=\min[\mu+\omega_D,\max(\epsilon_2)],$$

$$l_2=\max[\mu-\omega_D,\min(\epsilon_2)], \tag{28}$$

where $\max(\epsilon_2)$,$\min(\epsilon_2)$ is the maximun (minimum) of the two-dimensional band. In spite of the numerical simplification, for each one of the figures presented (Figs. 2 and 3), we spend 3 h for going from $\rho=0.01$ to $\rho=0.90$ in steps of $\delta\rho=0.01$.

From Figs. 2 and 3 we observe that the minimum value of the isotope exponent (upper panel, right scale) is around 0.5. At half filling, i.e., $\rho=1/2$, $\alpha\approx 0.3$–3.5, which is close to the experimental value of α for MgB_2. This result is almost independent of pairing interaction V. On the contrary, T_c changes with V and ω_D. As a consequence, the Debye frequency and the pairing potential are good parameters to tune the maximum value of the superconducting critical temperature. We also observe that for the maximum value of T_c, which occurs at half filling, there is a local minimum for the isotope exponent. This is due to the fact that at half filling the system feels the presence of the van Hove singularity. Also, we observe that there are two other local symmetric minima in α which are mostly likely due to the fine details of the three-dimensional band (see Fig. 3 of Ref. 47, for $\gamma=1$). In the lower panel, we have plotted α versus T_c, for V

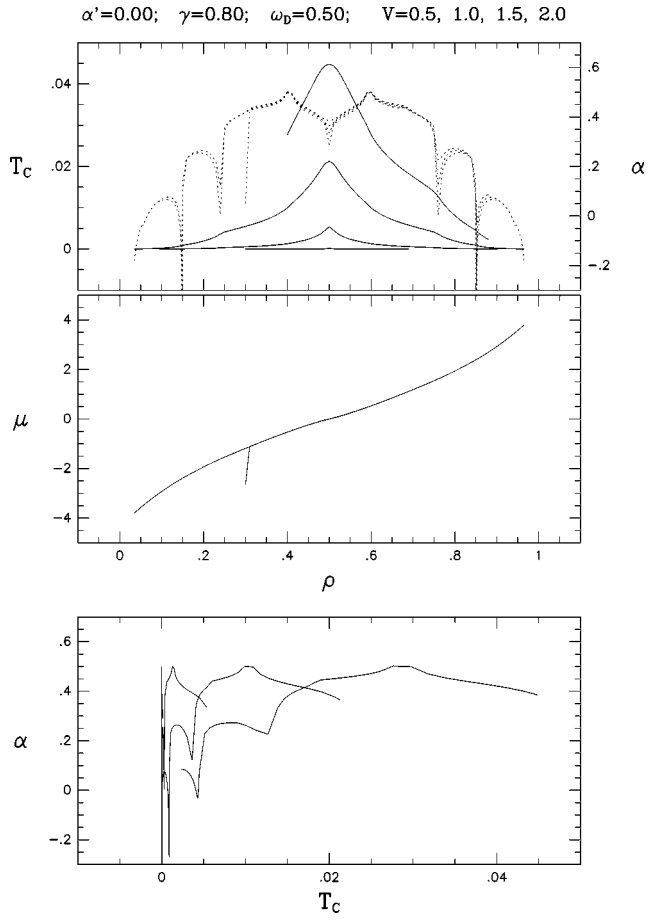

FIG. 4. The superconducting critical temperature T_c versus ρ, for several values of the attractive interaction V, namely, $V=0.5,1.0,1.5,2.0$ (upper panel, left scale) and the isotope exponent α versus ρ (upper panel, right scale). In the middle panel, we have the chemical potential, μ versus ρ, for the same values of the attractive interaction V. We have taken $\gamma=0.8$ and $\alpha'=0.0$ [see Eq. (17)]. Here, we have used a Debye frequency $\omega_D=0.50$.

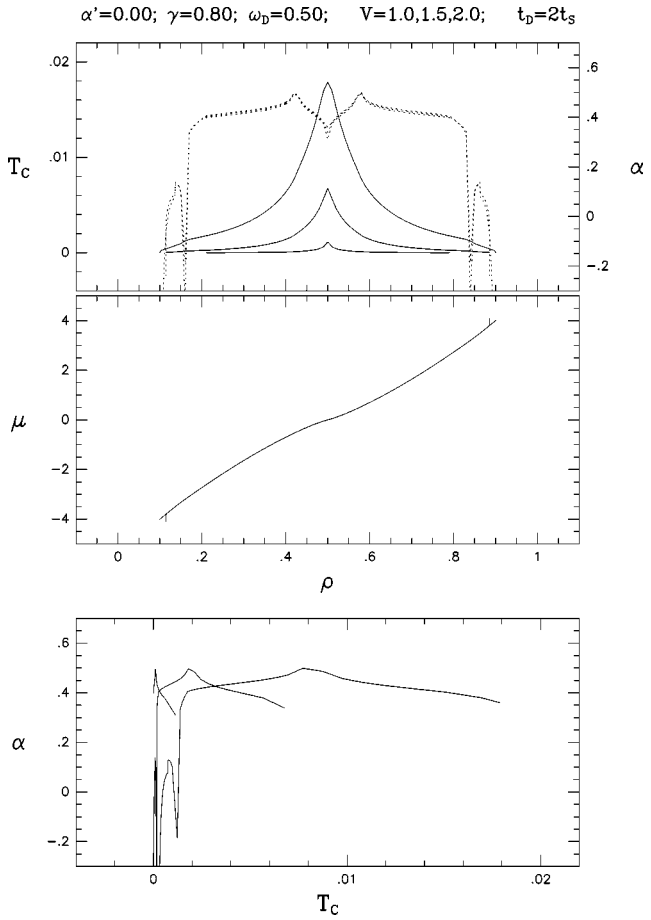

FIG. 5. The superconducting critical temperature T_c versus ρ, for several values of the attractive interaction V, namely, $V=1.0,1.5,2.0$ (upper panel, left scale) and the isotope exponent α versus ρ (upper panel, right scale). In the middle panel, we have the chemical potential μ versus ρ, for the same values of the attractive interaction V. We have taken $\gamma=0.8$ and $\alpha'=0.0$ [see Eq. (17)]. Here, we have used a Debye frequency $\omega_D=0.50$.

$=0.5,1.0,1.5,2.0$. We naturally see that the isotope exponent versus critical temperature is multivalued. We also observe that the two symmetric minima of the isotope exponent are located where the critical temperature changes curvature as function of ρ.

In order to explore the effects of the fine details of the three-dimensional band structure, in Fig. 4, we have chosen $\gamma=0.8$, $\omega_D=0.30$, and $\alpha'=0.0$. We observe that instead of two symmetric minima for α, around half filling, we have four symmetric minima for α around $\rho=1/2$.

From Figs. 1–4 we observe (intermediate panel) that the chemical potential is independent of pairing interaction, i.e., the curves stay one on top of each other.

C. Results using Eq. (20), with $t_3=2t_2$

To see the importance of $t_3\neq t_2$, which is implicit in the two Fermi surfaces presented by Mazin and Antropov,[49] we have tried a new set of parameters, namely, $t_3=2t_2$. This is shown in Fig. 5, for $\gamma=0.8$, $\omega_D=0.5$, and $V=1.0,1.5,2.0$. We have not plotted T_c versus ρ for $V=0.5$ because $T_c\approx 10^{-6}$ and we do not see it at all.

Now we compare Figs. 4 and 5. Both of them have the same set of parameters, except that for Fig. 4 $t_3=t_2$, while for Fig. 5 $t_3=2t_2$. We observe that the number of *oscillations* in the isotope exponent α goes down. This is a signature that the size of the Brillouin zone (or hopping) for the three-dimensional band is important. In addition, we also observe that T_c^{max} goes down with $t_3=t_D=t_d$.

If we increase the parameter γ, namely, $\gamma=1.0$, we have Fig. 6, where we have basically eliminated all the symmetric minima for the isotope exponent α. We also observe that $T_c\neq 0$ occurs mostly inside the two-dimensional band, for which $\mu\in(-4,4)$.

In short, we have calculated the superconducting critical temperature T_c versus ρ for a two-band superconducting, both with *s*-symmetry order parameter. Our Fig. 1 is highly symmetric around half filling, $\rho=1/2$. We have also studied the isotope exponent [see Eq. (21)]. In order to do this, we must use Eq. (20), where the presence of the Debye parameter enters. As MgB_2 belongs to a huge family of compounds and it holds the highest T_c, then we conclude that under our working scheme MgB_2 has a half-filling carrier density, if

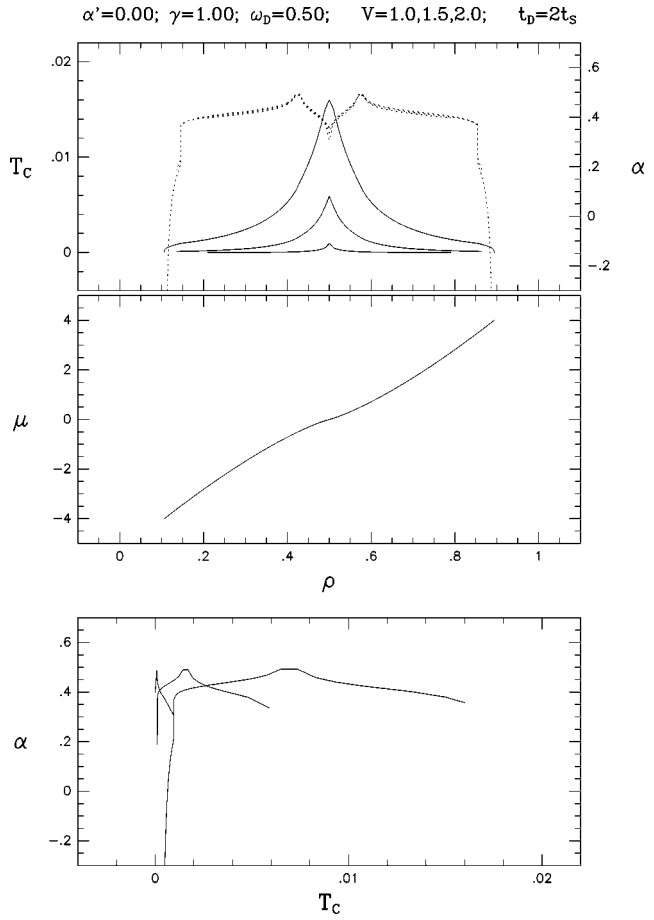

FIG. 6. The superconducting critical temperature T_c versus ρ, for several values of the attractive interaction V, namely, $V=1.0,1.5,2.0$ (upper panel, left scale) and the isotope exponent α versus ρ (upper panel, right scale). In the middle panel, we have the chemical potential μ versus ρ, for the same values of the attractive interaction V. We have taken $\gamma=1.0$ and $\alpha'=0.0$ [see Eq. (17)]. Here, we have used a Debye frequency $\omega_D=0.50$.

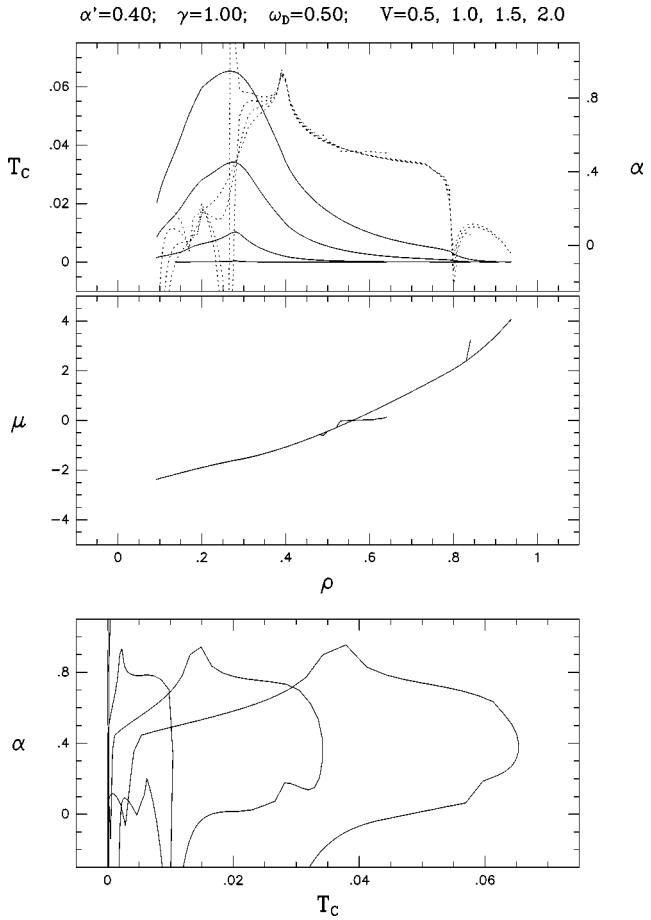

FIG. 7. The superconducting critical temperature T_c versus ρ, for several values of the attractive interaction, V, namely, $V=1.0,1.5,2.0$ (upper panel, left scale) and the isotope exponent α versus ρ (upper panel, right scale). In the middle panel, we have the chemical potential μ versus ρ, for the same values of the attractive interaction, V. We have taken $\gamma=1.0$ and $\alpha'=0.40$ [see Eq. (17)]. We have used $\omega_D=0.50$ and $t_2=t_3$.

$\alpha'=0$. Our Figs. 1–4 qualitatively show that T_c versus ρ curves are similar to the experimental curves of Tc versus x in Ref. 50, where $x=1-\rho$ is the excess of carbon fraction, i.e., for the compound $MgB_{2-x}C_x$. These results are in agreement with experimental work of Ref. 51. Also, for Mg substitution, T_c goes down with doping, namely, we have the compound $Mg_{1-y}D_yB_2$, where $D=$Li and Al, for example. For this case too T_c goes down with doping. This is in agreement with the results of Karpinski and co-workers.[52,53]

We have also considered $t_3 \neq t_2$ following Mazin and Antropov.[49] They have used LMT-ASA, full-potential linear muffin-tin orbital, or full-potential LAPW methods to study the band structures of AlB_2 structures. Their Fig. 3 shows the Fermi surface of MgB_2 which has been modeled by Dahm and Schopohl.[54] By taking two Fermi surfaces, one by half torus for the π band and another by a distorted cylinder for the σ band, they have been able to explain the upper critical magnetic-field anisotropy, $B_{c_2}^{ab}/B_{c_2}^{c}$ versus T, for $0 \leqslant T \leqslant T_c$.

Finally, in Fig. 7 we present T_c versus ρ, for several values of the attractive interaction V, namely, $V=1.0,1.5,2.0$ (upper panel, left scale) and the isotope exponent α versus ρ (upper panel, right scale). In the middle panel, we have the chemical potential μ versus ρ, for the same values of the attractive interaction V. We have taken $\gamma=1.0$ and $\alpha'=0.40$ [see Eq. (17)]. Here, we have used a Debye frequency $\omega_D=0.50$ and $t_2=t_3$. We see that the symmetry at half filling is destroyed. Also, the behavior of the isotope exponent is more complicated than the previous cases. At the present moment, we are calculating a set of parameters with $t_2=2t_3$ for $\alpha' \neq 0.0$.

We would like to end this work by saying that two-band effects on transport properties have to be considered. In particular, resistivity and thermal conductivity realized by Putti *et al.*[55] indicate that the π and σ bands conduct in parallel, with prevailing π conduction in clean samples and σ conduction in dirty samples. The authors of Ref. 55 consider that these results are in agreement with the hypothesis of Mazin *et al.*[56] Very recent experimental data by Yang *et al.*[57] has shown that T_c goes down with Al doping up to $x=0.4$, namely, $(Mg_{1-x}Al_x)B_2$.

In Sec. I we have said that our choice of $V_{22}=V_{33}=0$ may be considered as a possible realization of a two-band superconductor. However, Rayd *et al.*[58] have studied the two-band effects in the angular dependence of upper critical field H_{c_2} of MgB_2 single crystals. They conclude, among other things, that with a slight adjustment of some of the parameters supplied by band-structure calculations, good quantitative agreement is found between theory[59] and experiment yielding fundamental estimates of band-structure anisotropies and interband coupling strength. For example, in their Table I, they have chosen off-diagonal parameters twice as large as the ones supplied by band-structure calculations. They also state that no direct experimental probe of the off-diagonal coupling constants is available at present. Because of this, our choice appears to be justified.

ACKNOWLEDGMENTS

We are very grateful to J. Karpinski, K. Maki, I. Ţifrea, F. Bouquet, J. S. Brooks, W. E. Pickett, J. A. Budagosky-Marcilla, I. Bonalde, R. Medina, and H. Beck for interesting discussions. The numerical calculations were performed at LANA (Departamento de Matemática, UFSM). We thank CDCH-UC Venezuela (Project No. 2001-013) and FONACYT Venezuela for financial support (Grant No. S1-2002000448). This work was partially supported by the brazilian agencies FAPERGS and CNPq. One of the authors (J.J.R.N.) acknowledges financial support by Venezuelan Program of Scientific Research (P.P.I.-II). We thank M. D. García-González for helping us with the preparation of this paper.

*Electronic address: jjrn01@cantv.net
†Electronic address: alex@lana.ccne.ufsm.br

[1] T. Yildirim, Mater. Today **5** (4), 40 (2002).
[2] J. Nagamatsu, N. Nakagawa, T. Muranaka, Y. Zenitani, and J. Akimitsu, Nature (London) **410**, 63 (2001); T. Muranaka, J. Akimitsu, and M. Sera, Phys. Rev. B **64**, 020505(R) (2001); T. Takahashi, T. Sato, S. Souma, T. Muranaka, and J. Akimitsu, Phys. Rev. Lett. **86**, 4915 (2001).
[3] J.M. An and W.E. Pickett, Phys. Rev. Lett. **86**, 4366 (2001).
[4] T. Yildirim and O. J. Gulseren, J. Phys. Chem. (to be published).
[5] A.Y. Liu *et al.*, Phys. Rev. Lett. **87**, 087005 (2001).
[6] C. Joas, I. Eremin, D. Manske, and K.H. Bennemann, Phys. Rev. B **65**, 132518 (2002).
[7] H.J. Choi, D. Roundy, H. Sun, L. Cohen, and S.G. Louie, Nature (London) **418**, 15 (2002).
[8] H. Suhl, B.T. Matthias, and L.R. Walker, Phys. Rev. Lett. **3**, 552 (1959).
[9] J.B. Ketterson and S.N. Song, *Superconductivity* (Cambridge University Press, Cambridge, 1999).
[10] N. Kristoffel and T. Ôrd, cond-mat/0105536 (unpublished); N. Kristoffel and P. Rubin, Physica C **356**, 171 (2001).
[11] V.Z. Kresin, H. Morawitz, and S.A. Wolf, *Mechanisms of Conventional and High T_c Superconductivity* (Oxford University Press, Oxford, 1993).
[12] V.Z. Kresin and S.A. Wolf, *Fundamentals of Superconductivity* (Plenum Press, New York, 1990).
[13] J. Kortus, I.I. Mazin, K.D. Belashchenko, V.P. Antropov, and L.L. Boyer, Phys. Rev. Lett. **86**, 4656 (2001).
[14] M. Iavarone, G. Karapetrov, A.E. Koshelev, W.K. Kwok, G.W. Crabtree, and D.G. Hinks, cond-mat/0203329 (unpublished).
[15] M.-S. Kim, J.A. Skinta, and Th. Lemberger, cond-mat/0201550 (unpublished).
[16] G. Lamura, E. Di Gennaro, M. Salluzzo, A. Andreone, J. Le Cochec, A. Gauzzi, C. Cantoni, M. Paranthaman, D.K. Christen, H.M. Christen, G. Ciunchi, and S. Ceresra, Phys. Rev. B **65**, 020506(R) (2002).
[17] F. Bouquet, R.A. Fisher, N.E. Phillips, D.G. Hinks, and J.D. Jorgensen, Phys. Rev. Lett. **87**, 047001 (2001); F. Bouquet, Y. Wang, R.A. Fisher, D.G. Hinks, J.D. Jorgensen, A. Junov, and N.E. Phillips, Europhys. Lett. **56**, 856 (2001).
[18] F. Manzano, A. Carrington, N.E. Hussey, S. Lee, A. Yamamoto, and S. Tajima, Phys. Rev. Lett. **88**, 047002 (2002); cond-mat/0110109 (unpublished).
[19] A.B. Kuz'menko, F.P. Mena, H.J.A. Molegoraaf, D. van der Marel, B. Gorshunov, M. Dresnel, I.I. Mazin, J. Kortus, O.V. Dolgov, T. Muranaka, and J. Akimitsu, Solid State Commun. **121**, 479 (2002).
[20] A. Dulcic, D. Paar, M. Pozek, G.V.M. Williams, S. Krämer, C.U. Jung, M.S. Park, and S.I. Lee, Phys. Rev. B **66**, 014505 (2002).
[21] K. Yamaji, J. Phys. Soc. Jpn. **70**, L1476 (2001).
[22] N. Furukawa, cond-mat/0103184 (unpublished); J. Phys. Soc. Jpn. **70**, L1483 (2001).
[23] N. Nakai, M. Ichioka, and K. Machida, J. Phys. Soc. Jpn. **71**, L23 (2001).
[24] S. Haas and K. Maki, Phys. Rev. B **65**, 020502(R) (2002).
[25] T.M. Mishonov, E.S. Penev, and J.O. Indekeu, cond-mat/0204545 (unpublished).
[26] A.Y. Liu, I.I. Mazin, and J. Kortus, Phys. Rev. Lett. **87**, 087005 (2001); A.A. Golubov, A. Brinkman, O.V. Dolgov, J. Kortus, and O. Jepsen, cond-mat/0205154 (unpublished).
[27] C.P. Moca, Phys. Rev. B **65**, 132509 (2002).
[28] C. Panagopoulos, B.D. Rainford, T. Xiang, C.A. Scott, M. Kantara, and I.H. Inoue, Phys. Rev. B **64**, 094514 (2001).
[29] M. Pissas, S. Lee, A. Yamamoto, and S. Tajima, cond-mat/0205561 (unpublished); Yu. Eltsev, K. Nakao, S. Lee, T. Misui, N. Chikumoto, S. Tajima, N. Koshizuka, and M. Muramaki, cond-mat/0204027 (unpublished).
[30] O.F. de Lima, C.A. Cardoso, R.A. Ribeiro, M.A. Avila, and A.A. Coelho, Phys. Rev. Lett. **86**, 5974 (2001).
[31] C. Buzea and T. Yamashita, cond-mat/0108265 (unpublished); Semicond. Sci. Technol. **14**, R115 (2001).
[32] C.M.I. Okoye, Chin. J. Nucl. Phys. (Taipei) **36**, 53 (1998).
[33] S.V. Shulga, S.-L. Drechsler, G. Fuchs, K.-H. Müller, K. Winzer, M. Heinecke, and K. Krug, Phys. Rev. Lett. **80**, 1730 (1998).
[34] D.F. Agterberg, T.M. Rice, and M. Sigrist, Phys. Rev. Lett. **78**, 3374 (1997); D.F. Agterberg, Phys. Rev. B **60**, 749(R) (1999).
[35] A.V. Sologubenko, J. Jun, S.M. Kazakov, J. Karpinski, and H.R. Ott, cond-mat/0201517 (unpublished); Phys. Rev. B **66**, 014504 (2002).
[36] N.N. Bogoliubov, J. Exp. Theor. Phys. **34**, 65 (1958) [Sov. Phys. JETP **7**, 41 (1958)]; Nuovo Cimento **7**, 794 (1958); J.G. Valatin, *ibid.* **7**, 843 (1958).
[37] See, for example, A.L. Fetter, and J.D. Walecka, *Quantum Theory of Many-Particle Systems* (McGraw-Hill, New York, 1971).

[38] G.D. Mahan, *Many-Particle Physics*, 3rd ed. (Plenum Press, New York, 2000).
[39] J.J. Rodríguez-Núñez and J.A. Budagosky-Marcilla (unpublished).
[40] I. Ţifrea, J.A. Budagosky-Marcilla, and J.J. Rodrıguez-Núñez, Phys. Rev. B **66**, 104507 (2002); J.J. Rodríguez-Núñez, J.A. Budagosky-Marcilla, and I. Ţifrea, Acta Phys. Pol. B **46**, 383 (2003).
[41] E.L.V. de Mello and J.J. Rodríguez-Núñez, Physica C **365**, 144 (2001).
[42] S.K. Bud'ko, G. Lapertot, C. Petrovic, C.E. Cunningham, N. Anderson, and P.C. Canfield, Phys. Rev. Lett. **86**, 1877 (2001).
[43] A. Bill, V.Z. Kresin, and S.A. Wolf, http://people.web.psi.ch/bill/ISOTOPE/reviewIE.pfd; cond-mat/9801222 (unpublished); *Pair Correlations in Many-Fermion Systems* (Plenum Press, New York, 1998), p. 25. See also, V.Z. Kresin, A. Bill, S.A. Wolf, and Yu.N. Ovchinnikov, Phys. Rev. B **56**, 107 (1997); A. Bill, V.Z. Kresin, and S.A. Wolf, *ibid.* **57**, 10814 (1998); Z. Phys. B: Condens. Matter **104**, 759 (1997).
[44] H. Kusunose, T.M. Rice, and M. Sigrist, cond-mat/0208113 (unpublished).
[45] M.B. Soares, F. Kokubun, J.J. Rodríguez-Núñez and O. Rendón, Phys. Rev. B **65**, 174506 (2002); see also, A. Perali, P. Pieri, G.C. Strinati, cond-mat/0211132 (unpublished); Phys. Rev. B **68**, 066501 (2003); J.J. Rodríguez-Núñez, O. Alvarez-Llamoza, E. Orozco, O. Rendón, D. Kokubun, and M.B. Soares, *ibid.* **68**, 066502 (2003).
[46] W.L. McMillan, Phys. Rev. **167**, 331 (1968).
[47] K. Pesz and R.W. Munn, J. Phys. C **19**, 2499 (1986).
[48] J. Kishine, Prog. Theor. Phys. **94**, 543 (1995).
[49] I.I. Mazin and V.P. Antropov, cond-mat/0212263 (unpublished); See also, S.V. Shulga, S.-L. Drechsler, H. Eschrif, H. Rosner, and W. Pickett, cond-mat/0103154 (unpublished); S.V. Shulga and S.-L. Drechsler, cond-mat/0202172 (unpublished).
[50] S. Jemina Balaselvi, A. Bharathi, V. Sankara Sastry, G.L.N. Reddy, and Y. Hariharam, cond-mat/0209200 (unpublished); cond-mat/0303033 (unpublished).
[51] S.M. Kazakov, J. Karpinski, J. Jun, P. Geiser, N.D. Zhigadlo, R. Puzniak, and A.V. Mironov, cond-mat/0304656 (unpublished).
[52] J. Karpinski, S.M. Kazakov, J. Jun, N.D. Zhigadlo, M. Angst, R. Puzniak, and A. Wisniewski, cond-mat/0304658 (unpublished); J. Karpinski (private communication).
[53] J.Q. Li, L. Li, F.M. Liu, C. Dong, J.Y. Xiang, and Z.X. Zhao, cond-mat/0104320 (unpublished).
[54] T. Dahm and N. Schopohl, cond-mat/0212188 (unpublished).
[55] M. Putti, V. Braccini, E. Galleani, F. Napoli, I. Pallecchi, A.S. Siri, P. Manfrinetti, and A. Palenzola, Semicond. Sci. Technol. **16**, 188 (2003); Phys. Rev. B **67**, 064505 (2003).
[56] I.I. Mazin, O.K. Andersen, O. Jepsen, O.V. Dolgov, J. Kortus, A.A. Golubov, A.B. Kuz'menko, and D. van der Marel, cond-mat/0204013 (unpublished); Phys. Rev. Lett. **89**, 107002 (2002).
[57] H.D. Yang, H.L. Liu, J.-Y. Liun, M.X. Kuo, P.L. Ho, J.M. Chen, C.V. Jung, M.-S. Park, and S.-I. Lee, cond-mat/0308081 (unpublished).
[58] A. Rydh, U. Welp, A.E. Koshelev, W.K. Kowk, G.W. Crabtree, R. Brusetti, L. Lyard, T. Klein, C. Marcenat, B. Kang, K.H. Kim, K.H. Kim, H.-S. Lee, and S.-I. Lee, cond-mat/0308319 (unpublished).
[59] A.A. Golubov and A.E. Koshelev, cond-mat/0303237 (unpublished).